



Thrust Chamber Dynamic and Propulsive Performance of Biofuels Under Detonation Combustion

Izham Izzat Ismail¹, Muhammad Hanafi Azami^{1,*}

¹ Department of Mechanical & Aerospace Engineering, Faculty of Engineering, International Islamic University Malaysia, Kuala Lumpur, Malaysia

ARTICLE INFO

Article history:

Received 3 October 2021
Received in revised form 9 December 2021
Accepted 15 December 2021
Available online 18 February 2022

Keywords:

Pulse Detonation Engines (PDE);
Alternative Fuels; Propulsive
Performance

ABSTRACT

Detonation is a shock wave obtained from the energy that releases after the combustion. Chapman-Jouguet (CJ) theory can be used to identify the behaviour of the detonation in gasses. Pulse Detonation Engines (PDEs) is one of the engines that implement the detonation in its combustion system. The Humphrey cycle is the thermodynamic cycle which is similar to the Pulse Detonation Engines (PDEs). It is the modification of the Brayton cycle where the constant-pressure heat addition process of the Brayton cycle is replaced by a constant-volume heat addition process. The Humphrey cycle can provide the pressure rise combustion by utilizing the shock inside the combustion chamber. Compared to the Brayton cycle, the Humphrey cycle has higher thermodynamic efficiency. However, the detonation process has unsteady combustion which makes it more difficult to handle. The purpose of the study is to calculate the performance of the aircraft by using alternative fuel in the ZND model. An analytical model is started by having the molecular structure of each biofuel and it has been used to determine detonation velocity, Mach number at C-J point, temperature ratio, pressure ratio, density ratio, Brayton and Humphrey efficiency, specific impulse, and specific thrust. In addition, the physical properties of the flow are investigated by changing the initial temperature, initial pressure, and mass flux. The pressure ratio, temperature ratio, and density ratio will all decrease as the initial pressure varies. The variation of mass flux and initial temperature, on the other hand, generates the opposite outcome as the change of pressure. The feasibility of the fuels in the detonation combustion can be known as they show high propulsive performance after the initial condition is changing.

1. Introduction

Pulse Detonation Engines (PDEs) becoming popular among researchers. The number of researchers keeps on increasing as it gives the advantage in terms of thermodynamic cycle efficiency, hardware simplicity, and operation scalability and reliability [1-4]. However, there is some challenge that is faced during applying the Pulse Detonation Engines (PDEs) in the aircraft.

One of the challenges is to integrate the inlet with the unsteady-operated detonation chamber and to choose an optimized nozzle to achieve high performance [5]. The performance of the Pulse

* Corresponding author.

E-mail address: hanafiazami@iium.edu.my

<https://doi.org/10.37934/arfmts.92.2.7193>

Detonation Engines (PDEs) can be estimated by using theoretical and numerical attempts. Pulse detonation engines (PDEs) are different from conventional as this engine is producing thrust by using repetitive propagating detonation [6]. Humphrey cycle analysis has been implemented in the Pulse detonation engines (PDEs) as it increased the thermodynamic efficiency of the aircraft [7]. By calculating the area under the graph, it shows that the Humphrey cycle is producing better performance than the Brayton cycle.

In this paper, the feasibility of biofuels is going to be investigated. These biofuels are going to be implemented in Pulse detonation engines (PDEs). To predict the propulsive performance of the aircraft, the theoretical and numerical method is being used to calculate specific impulses, specific thrust, and also the efficiency of aircraft. The calculation will give the comparison for all biofuels that have been investigated. Although biofuels are reducing thermodynamic potency and performance, it provides other advantages by reducing global emissions of carbon dioxide [8], [9]. Implementing biofuels in the PDEs is one of the efforts that can be done to provide an aircraft with a better performance.

The pulse detonation engine is one of the engines that use the detonation wave to combust the oxidizer mixture with the fuel. The thrust is generated by using high pressure that is generated by repetitive detonation waves [10–12]. Between each detonation wave, the mixture is renewed and causes the engine to pulse. The detonation wave is initiated by an ignition source. The researchers have found that a Pulse detonation engine (PDE) can fly from subsonic to hypersonic speed. The detonation wave rapidly compresses the mixture and adds heat at constant volume to provide higher thermodynamic efficiency. Having a Pulse detonation engine (PDE) in the aircraft can increase fuel efficiency [13]. In addition, the thrust to weight ratio also is higher compared to a conventional engine. Pulse detonation engine (PDE) does not require a compressor and turbine in the engine operation [14]. Therefore, it will cut the cost of the aircraft and at the same time make the engine mechanical simpler and have a lightweight. The advantage and disadvantages of pulse detonation are shown in Table 1.

Table 1
Advantages and Disadvantages

| Advantages | Reference |
|--|-----------|
| High frequency | [15] |
| High specific impulse | [16] |
| High thermodynamic cycle efficiency | [2] |
| Low compression ratio | [17] |
| Improve fuel efficiency and longer range | [17] |
| Can be used in other developing technology | [17] |
| Less moving parts and low cost | [18] |
| Lower specific fuel consumption (SFC) | [19] |
| Disadvantages | Reference |
| Smaller takeoff thrust-to-weight | [19, 20] |
| Vibration and Noise | [20] |

2. Methodology

In this condition, the reacting gasses reach the sonic speed as the reaction end. According to [21] chemical reactions are modeled as a heat release in a thin shock front that brings the material from the initial state to the subsequent state [21]. It is known as CJ point [14]. In the real detonation is highly three-dimensional, considerable insight is provided by one-dimensional analysis. Figure 1 is

the first attempt to explain detonation accordingly by Chapman in 1899 which relied on a one-dimensional approach.

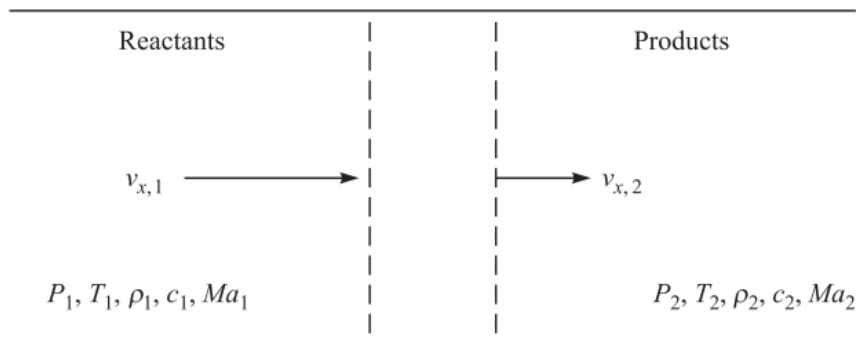


Fig. 1. One-dimensional detonation wave in a constant-area duct [22]

2.1 Assumption and Biofuel Properties

The assumption that has been made in this paper are (i) After including upstream and downstream boundaries, there are no temperature or species concentration gradients. (ii) It is in a uniform one-dimensional flow. (iii) Under adiabatic conditions where there is no heat loss to the surrounding. (iv) Negligible body force. (v) The process considers the normal shock relation. Many types of biofuels are used in aircraft. Table 2 shows the molecular weight for each alternative fuel used.

Table 2
 Alternative fuels characteristic

| Properties | Molecular Formula |
|-------------|-------------------|
| Jojoba | $C_{38}H_{76}O_2$ |
| Jatropha | $C_{12}H_{26}$ |
| Linseed oil | $C_{57}H_{98}O_6$ |
| Palm oil | $C_{16}H_{32}O_2$ |

2.2 Formation of Rayleigh line

Rayleigh relation is formed by combining the mass and momentum conservation as in Eq. (1). Then, Manipulations of all the conservation equations yield the following Hugoniot relation shown in Eq. (2).

$$\frac{p_2 - p_1}{\frac{1}{\rho_2} - \frac{1}{\rho_1}} = \frac{p_2 - p_1}{v_2 - v_1} = -\dot{m}''^2 \quad (1)$$

$$\frac{\gamma}{\gamma - 1} \left(\frac{p_2}{\rho_2} - \frac{p_1}{\rho_1} \right) - \frac{1}{2} (p_2 - p_1) \left(\frac{1}{\rho_2} + \frac{1}{\rho_1} \right) - q = 0 \quad (2)$$

$$v = \frac{1}{\rho} \quad (3)$$

Substitute Eq. (3) into Eq. (2), then all value of P_2 is substituted by using Eq. (1). Expanding and converting to the quadratic equation in terms of the v_2 :

$$av_2^2 + bv_2 + c = 0 \quad (4)$$

$$a = \frac{1 + \gamma}{2(1 - \gamma)} \dot{m}''^2 \quad (5)$$

$$b = \frac{\gamma}{\gamma - 1} (p_1 v_1 + \dot{m}''^2 v_1) \quad (6)$$

$$c = \frac{\gamma}{1 - \gamma} p_1 v_1 - \frac{1}{2} \dot{m}''^2 v_1^2 - q \quad (7)$$

Find the value for a, b and c by using the ideal gas equations. From the value of a, b and c solve for v_2 :

$$v_2 = \frac{-b \pm \sqrt{b^2 - 4ac}}{2a} \quad (8)$$

As the value of P_2 is solved, determine which solution lies on the Hugoniot and which region it refers to. Based on both velocity and local sound speed the Mach number is calculated. The value of $v_{x,2}$ is calculated from the mass flux equation.

$$v_{x,2} = \dot{m}''^2 v_2 \quad (9)$$

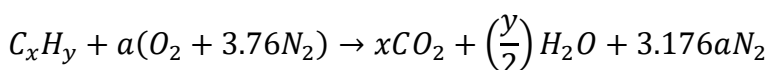
To calculate the sound speed, determine the state-2 temperature. It can determine from the ideal gas equation of state. Therefore, used the value of T_2 determine the speed of sound. Then, from the value of C_2 , calculate the value of M_2 .

$$c_2 = (\gamma_2 R_2 T_2)^{\frac{1}{2}} \quad (10)$$

$$v_{x,2} = \dot{m}''^2 v_2 \quad (11)$$

2.3 Detonation Velocity

By using Appendix A in [23], the unreacted mixture specific heat can be obtained. Before start finding these properties, determine the composite of the unreacted and reacted mixtures.



Balance the equation on the left side and the right side. As the equation has been balanced, find the thermochemical properties by using the formula below. Then, calculate the specific heat for states 1 and 2:

$$C_{p,n} = \frac{\sum_{state,n} X_i \hat{c}_{p,n}}{MW_n} \quad (12)$$

By using the gas constant formula get the value of R_2 and calculate the Specific heat ratio.

$$\gamma_2 = \frac{C_{p,2}}{C_{v,2}} = \frac{C_{p,2}}{C_{p,2} - R_2} \quad (13)$$

By referring to appendix A, enthalpies-of-formation can be obtained to calculate Heat formation, q . Enthalpies-of-formation is converted to a mass basis. Then Detonation velocity and temperature at state 2 can be calculated by using the formula Eq. (15) and Eq. (16):

$$q \equiv \sum_{state1} Y_i h_{f,i}^0 - \sum_{state2} Y_i h_{f,i}^0 \quad (14)$$

$$v_D = \left[2\gamma_2 R_2 (\gamma_2 + 1) \left(\frac{\hat{c}_{p,1}}{\hat{c}_{p,2}} T_1 + \frac{q}{\hat{c}_{p,2}} \right) \right]^{\frac{1}{2}} \quad (15)$$

$$T_2 = \frac{2\gamma_2^2}{\gamma_2 + 1} \left(\frac{\hat{c}_{p,1}}{\hat{c}_{p,2}} T_1 + \frac{q}{\hat{c}_{p,2}} \right) \quad (16)$$

By following the ideal-gas normal-shock equation, properties at state 2' can be determined. These properties are used to compare with properties at state 1 and state 2. The value of mixture specific heat ratio and the Mach number at state 1 is required to calculate all the properties at state 2'. It can be calculated by using the equation below. Assume $\gamma=1.3$ and calculate Mach number at state 1.

$$M_{a1} = \frac{V_{x1}}{C_1} = \frac{V_{x1}}{\sqrt{\gamma R_1 T_1}} \quad (17)$$

After obtaining the value for Mach number at state 1 and mixture specific heat ratio, all properties at state 2' can be calculated using the formula below:

$$\frac{P_{2'}}{P_1} = \frac{1}{\gamma + 1} (2\gamma Ma_1^2 - (\gamma - 1)) \quad (18)$$

$$\frac{T_{2'}}{T_1} = (2 + (\gamma - 1)Ma_1^2) \frac{2\gamma Ma_1^2 - (\gamma - 1)}{(\gamma + 1)^2 Ma_1^2} \quad (19)$$

$$\frac{\rho_{2'}}{\rho_1} = \frac{(\gamma + 1)Ma_1^2}{(\gamma + 1)Ma_1^2 + 2} \quad (20)$$

The Mach number at state 2' and state 2 also be calculated to investigate the motion of aircraft whether it is in subsonic or supersonic.

$$V_{x,n} = \frac{\rho_1}{\rho_n} V_{x,1} \quad (21)$$

$$M_{a,n} = \frac{V_{x,n}}{\sqrt{\gamma_n R_n T_n}} \quad (22)$$

2.4 Humphrey and Brayton Efficiency

According to [22], thermodynamic cycle efficiency is the percentage of the heat release from a chemical reaction that is converted to kinetic energy.

$$n_H = 1 - \gamma \frac{T_2}{T_3} \frac{\left(\left(\frac{T_4}{T_3} \right)^{\frac{1}{\gamma}} - 1 \right)}{\left(\frac{T_4}{T_3} - 1 \right)} \quad (23)$$

$$n_B = 1 - \left(\frac{1}{\pi_c} \right)^{\frac{\gamma-1}{\gamma}} \left(\frac{1}{1 + M_\infty^2 \left(\frac{\gamma-1}{2} \right)} \right) \quad (24)$$

2.5 Specific Thrust, f_{sp} and Specific Impulse, I_{sp}

Determine the total temperature $Tt1$ and pressure $Pt1$ at the combustor entrance from the inlet flow analysis, which this value is obtained from [22]. Static temperature $T1$ and pressure $P1$ of reactants for a given filling Mach number $M1$ can be obtained by using the formula below Eq. (25) and Eq. (26). Then Find temperature $T2$ and pressure $P2$ at CJ point.

$$T_1 = \frac{Tt1}{1 + \frac{(\gamma_1 - 1)M_1^2}{2}} \quad (25)$$

$$P_1 = \frac{Pt1}{\left(1 + \frac{(\gamma_1 - 1)M_1^2}{2} \right)^{\frac{\gamma_1}{\gamma_1 - 1}}} \quad (26)$$

$$T_2 = T_1 \frac{R_1 \gamma_2}{R_2 \gamma_1} \left(\frac{1 + \gamma_1 M_D^2}{(1 + \gamma_2) M_D} \right)^2 \quad (27)$$

$$P_2 = P_1 \frac{(1 + \gamma_1 M_D^2)}{1 + \gamma_2} \quad (28)$$

Calculate the exit temperature by assuming isentropic flow expansion from the CJ state to the exit plane.

$$T_e = T_2 \left(\frac{P_\infty}{P_2} \right)^{\frac{\gamma_2 - 1}{\gamma_2}} \quad (29)$$

The energy balance is applied to deduce the exit velocity between the combustor entrance and the nozzle exit. Then, calculate the specific thrust and impulse:

$$u_e = \sqrt{2(q - (c_{p2}T_e - c_{p1}T_{t1}))} \quad (30)$$

$$F_{sp} = (1 + f)u_e - u_\infty \quad (31)$$

$$I_{sp} = \frac{F_{sp}}{fg} \quad (32)$$

If the purging process includes the exit temperature will be different. In the new exit temperature, we need to include cycle time, fill time, and open time.

$$T_e = \frac{T_{e1}\tau_{purge} + T_{e2}\tau_{fill}}{\tau_{open}} \quad (33)$$

Find the value for temperature exit at unburnt gas and CJ point which is T_{e1} and T_{e2}

$$T_{e1} = T_1 \frac{P_\infty^{\frac{\gamma_\infty - 1}{\gamma_\infty}}}{P_1} \quad (34)$$

$$T_{e2} = T_2 \frac{P_\infty^{\frac{\gamma_2 - 1}{\gamma_2}}}{P_2} \quad (35)$$

Find heat addition and fuel-to-air mass ratio.

$$\bar{q} = q \frac{\tau_{fill}}{\tau_{open}} \quad (36)$$

$$f_{new} = f \frac{\tau_{fill}}{\tau_{open}} \quad (37)$$

Find exit velocity by substituting new heat addition and new exit temperature

$$u_e = \sqrt{2(\bar{q} - (c_{p2}T_e - c_{p1}T_{t1}))} \quad (38)$$

Obtain the specific thrust and specific impulse by using the new value of the fuel-to-air mass ratio.

$$F_{sp\ new} = (1 + f_{new})u_e - u_\infty \quad (39)$$

$$I_{sp} = \frac{F_{sp\ new}}{fg} \quad (40)$$

3. Result and Discussion

3.1 Thermodynamics Parameters

To predict the detonation velocity, specific thrust, specific impulse, and other properties the thermodynamic parameter should be collected and interpreted. The biofuel that going to be used, makes the simple chemical relation in combustion. In this relation, the product of the combustion will be carbon dioxide, water, and nitrogen gas. To estimate the detonation velocity of our aircraft, the value of heat addition burned properties, and unreacted mixture specific heat should be estimated. First of all, we need to determine the composition of the reacted and unreacted mixture. From this composition, balance the product and reactant. After balancing the stoichiometric combustion, the species mole and mass fraction can be calculated. The thermochemical properties are tabulated in Table 3.

Table 3
 Thermochemical properties for all biofuels

| Reactant | | | | |
|------------|---------|----------|-------------|----------|
| Properties | Jojoba | Jatropha | Linseed oil | Palm oil |
| C_{P1} | 1.15 | 1.07 | 1.07 | 1.13 |
| γ_1 | 1.31 | 1.34 | 1.33 | 1.31 |
| Product | | | | |
| Properties | Jojoba | Jatropha | Linseed oil | Palm oil |
| C_{P2} | 1.50 | 1.51 | 1.49 | 1.51 |
| γ_2 | 1.24 | 1.24 | 1.24 | 1.24 |
| R_2 | 0.29 | 0.29 | 0.29 | 0.29 |
| T_2 | 2921.82 | 2623.62 | 2868.02 | 2928.18 |

Based on Table 3 shows that the alternative fuel needs very high heat addition to complete the combustion. This high heat addition is required to break the complex molecular structure of biofuels.

3.1.1 Detonation velocity

After calculating the thermochemical properties, the value of detonation velocity for each biofuel can be calculated. In theory, detonation velocity is the velocity at which the shock wavefront travels through a detonated explosive. Table 4 shows which biofuel that have the highest detonation velocity. In this calculation, Jojoba shows the highest value of detonation velocity which explained that this biofuel is the most difficult to detonate compared with other biofuels.

Table 4
 Detonation Velocity

| Properties | Detonation Velocity, V_d |
|-------------|----------------------------|
| Jojoba | 1848.13 |
| Jatropha | 1755.25 |
| Linseed oil | 1758.53 |
| Palm oil | 1777.16 |

3.1.2 Validation of burned gas states in a detonation

In the burn gas state, it will show two values of Mach number. One of the Mach numbers will lie in the weak detonation region in which the velocity is moving in a supersonic. Whereas the second Mach number will represent the strong Mach number in which the velocity will be subsonic. By referring to the book introduction to combustion [23], the fuel that has been used is acetylene and the Mach number that has been calculated is showed that 2.09 and 0.55. Table 5 illustrate the characteristic of each region in the Hugoniot curve. Based on Table 6, it is proved that the value of Mach number calculated is in subsonic and supersonic flow.

Table 5
 Physical phenomena of the Huguenot curve in a different segment adapted from the book introduction to combustion [23]

| The region of the Hugoniot Curve | Characteristic | Burn gas velocity, $v_{x,2}$ |
|----------------------------------|---------------------|------------------------------|
| Above D | Strong detonation | Subsonic |
| D-B | Weak detonation | Supersonic |
| B-C | Inaccessible | - |
| C-E | Weak deflagration | Subsonic |
| Below E | Strong deflagration | Supersonic |

Based on Table 6, it is proved that the value of Mach number calculated is in subsonic and supersonic flow biofuels.

Table 6
 Validation of the model in two segments

| Mach Number, M_2 | Properties | | | |
|--------------------|------------|----------|-------------|----------|
| | Jojoba | Jatropha | Linseed oil | Palm oil |
| Subsonic | 0.59 | 0.58 | 0.60 | 0.59 |
| Supersonic | 1.97 | 2.01 | 1.94 | 1.96 |

3.1.3 Different phase in detonation tube

By using the selected biofuel, there are three parameters have been analyzed and compared due to pressure ratio, density ratio, and temperature ratio. Table 7 and Figure 2 below are one of the results that have been collected from Jojoba oil biodiesel.

Table 7
 Change of jojoba oil biodiesel at different state

| Property | State 1 | State2' | State2 |
|---------------|---------|---------|--------|
| ρ/ρ_1 | 1.00 | 6.36 | 1.81 |
| P/P_1 | 1.00 | 36.57 | 18.85 |
| T/T_1 | 1.00 | 5.75 | 9.75 |

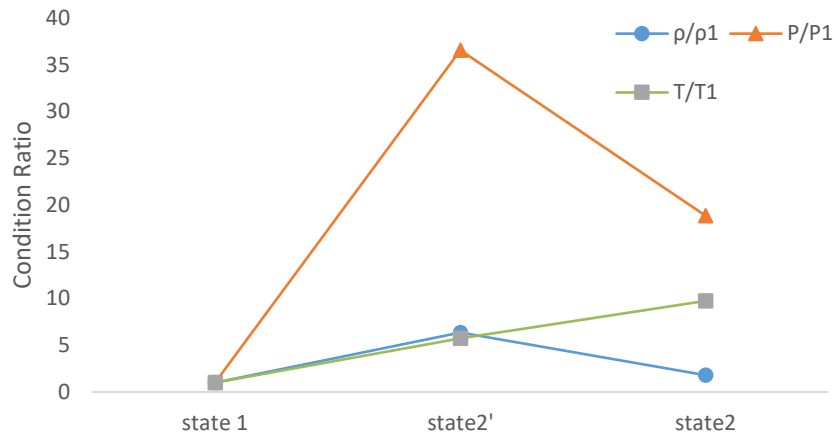


Fig. 2. Parameters changes at a different state

From the result that has been collected, the pressure ratio and density ratio across the initial shock front is very high, which are 6.36 and 36.57. The Mach number also shows that the flow is subsonic after the shock front (state2') and then accelerates to the sonic point at the trailing edge of the detonation wave (state2).

3.1.4 Detonation analysis pattern using ZND model

By comparing the various type of alternative fuels, it will prove which biofuels are going to show the best result. In the figure and table below, all biofuels that have been used are showing the same trend of increasing and decreasing across the state that we investigate. The result shows the highest pressure ratio in the shocking segment. The value of the high-pressure ratio for all biofuels shows that these biofuels are hardly distinguished and show almost the same reading.

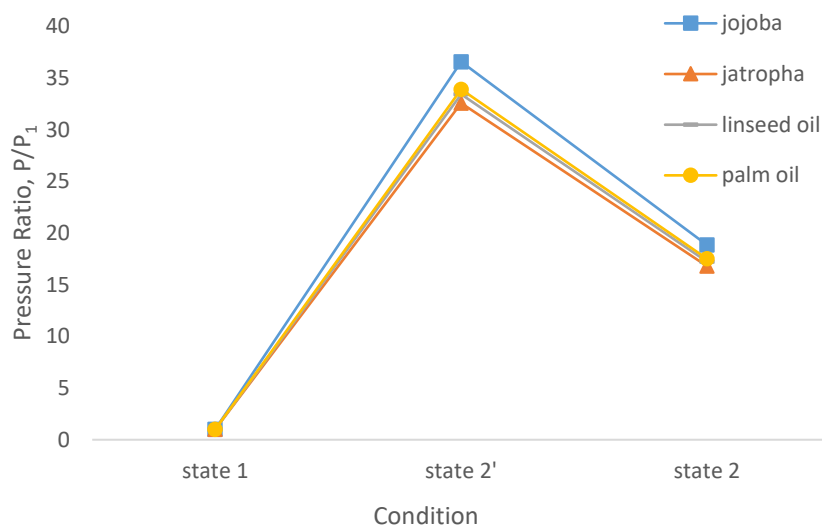


Fig. 3. Pressure ratio at different states

Table 8
 Pressure ratio

| Condition | Jojoba | Jatropha | Linseed oil | Palm oil |
|-----------|------------|-------------|-------------|-------------|
| state 1 | 1 | 1 | 1 | 1 |
| state 2' | 36.5651411 | 32.56034708 | 33.41736425 | 33.90069236 |
| state 2 | 18.8540686 | 16.797901 | 17.24260579 | 17.49504515 |

Next, the performance of the aircraft is determined by looking at the trend of the temperature ratio. The collected data shows that the temperature ratio is increasing along the detonation tube. Figure 4 shows that the temperature ratio is increasing significantly before the shock, then it continues to rise until the detonation wave. Similar to the pressure ratio, the temperature ratio for all fuels does not show a big difference between each other. It is clear that Jojoba fuels remain on the top after the shock takes place.

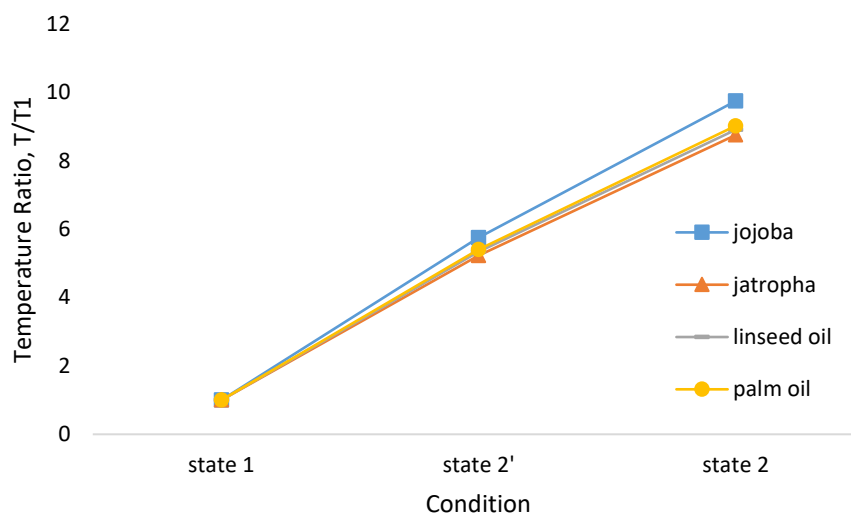


Fig. 4. Temperature ratio at different conditions

Table 9
 Temperature ratio

| Condition | Jojoba | Jatropha | Linseed oil | Palm oil |
|-----------|-------------|-------------|-------------|-------------|
| state 1 | 1 | 1 | 1 | 1 |
| state 2' | 5.748858962 | 5.226066487 | 5.337951529 | 5.401048605 |
| state 2 | 9.746388006 | 8.751871104 | 8.906468958 | 9.021007053 |

As presented in Figure 5, the density ratio demonstrates a similar trend to the pressure ratio. However, the highest value of fuels cannot be seen clearly. This is because the density ratio of all fuels only shows a small difference. Compared to the temperature ratio and pressure ratio, the reading of the density ratio at the detonation wave is not very significant. The reading of Jojoba oil fuel shows the highest reading in all three graphs. This result is due to the molecular structure of the Jojoba and the enthalpy formation of the reaction.

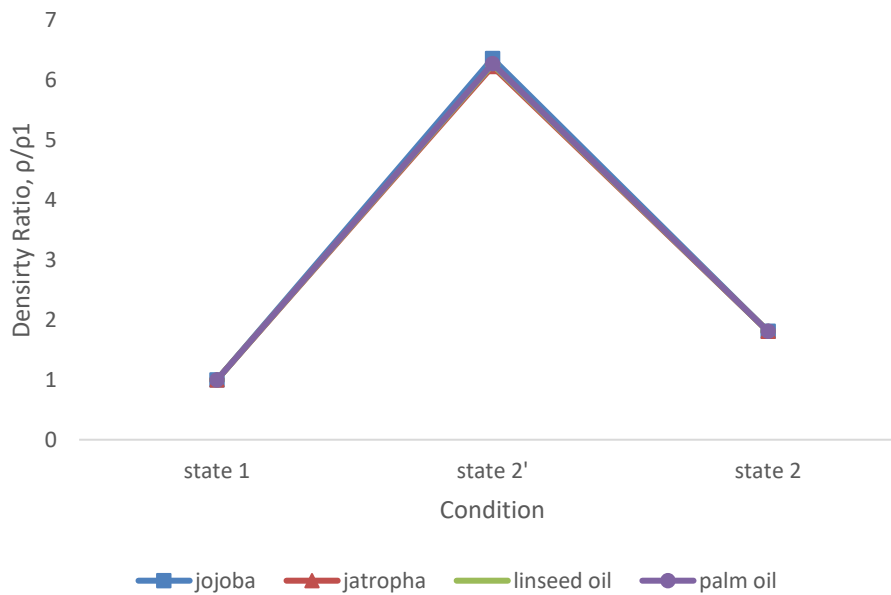


Fig. 5. Density ratio at different conditions

Table 10
 Density ratio

| Condition | Jojoba | Jatropa | Linseed oil | Palm oil |
|-----------|-------------|-------------|-------------|-------------|
| state 1 | 1 | 1 | 1 | 1 |
| state 2' | 6.360417144 | 6.230373679 | 6.2603349 | 6.276687146 |
| state 2 | 1.807598512 | 1.807727382 | 1.808094501 | 1.80843059 |

3.2 Changing of Initial Condition

In this part, this paper will discuss the impact of the various initial condition on the pressure ratio, temperature ratio, and density ratio. There are three variants of the initial condition that is going to be implemented to see the change of the parameter.

3.2.1 Various mass flux

By varying the value of mass flux, the value of pressure, density, temperature, and Mach number at the detonation wave will be affected. This parameter is calculated by using the mathematical approach and the result shows that the pattern of increasing and decreasing for all these parameters is the same. Figure 9 indicates that only the Mach number ratio is decreasing as the mass flux is increased. In addition, the temperature, density, and pressure ratio are showing the increasing result. Furthermore, the density, temperature, and pressure ratio of Jatropa are the highest followed by Jojoba and Linseed oil. However, the result shows that Jatropa has the lowest Mach number ratio. All biofuels only show small differences between each other.

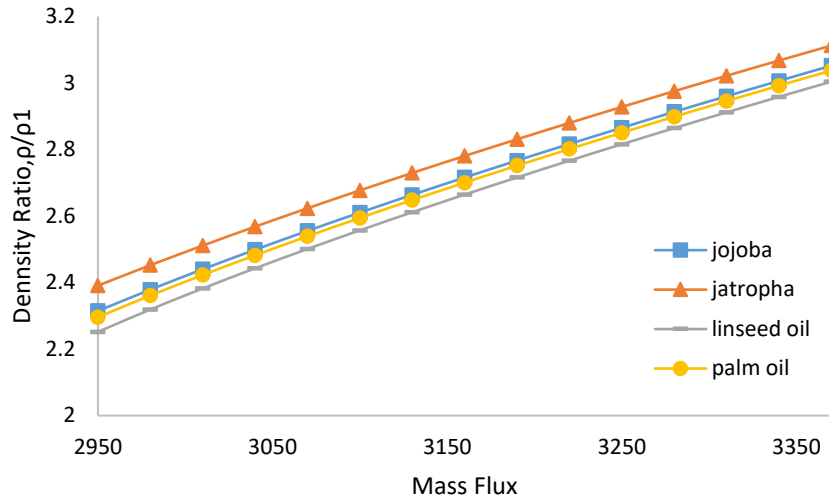


Fig. 6. Density ratio with different mass flux

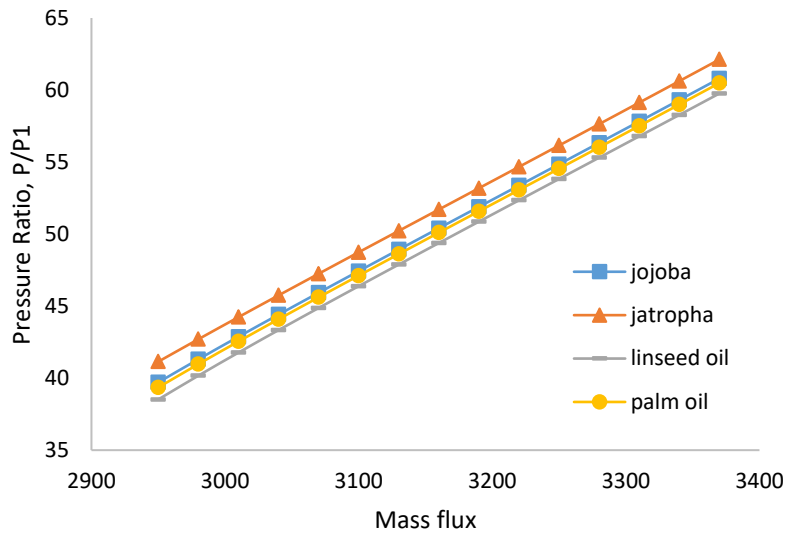


Fig. 7. Pressure ratio with different mass flux

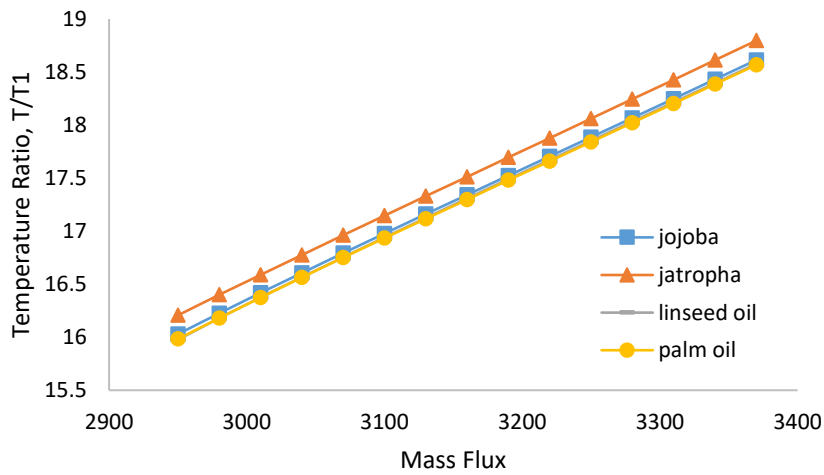


Fig. 8. Temperature ratio with different mass flux

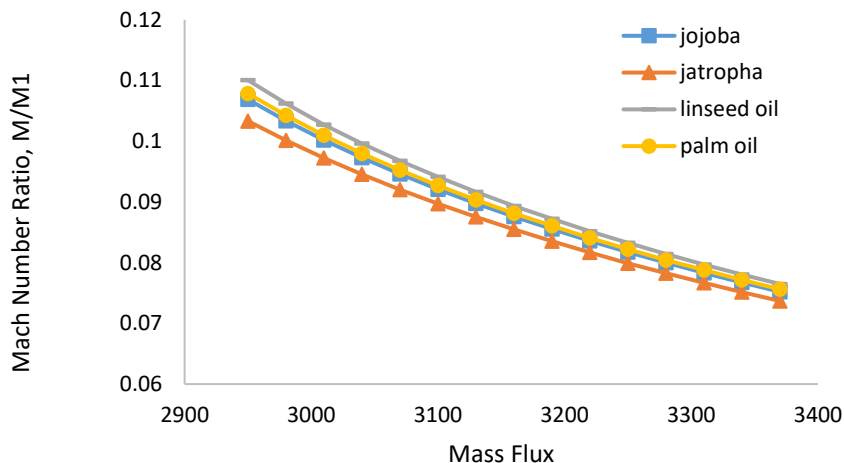


Fig. 9. Mach number ratio with different mass flux

3.2.2 Various initial temperature

The initial temperature of the fuel is varied to see the change of the temperature, density, pressure, and Mach number ratio. In this part, the mass flux and the initial pressure is going to be fixed. In this research, the initial temperature varies from 300 K to 2140K. Figure 10 shows that the density ratio of palm oil and jojoba increases significantly after the initial temperature is increasing. However, in the pressure and temperature ratio, all fuel decreases similarly without much difference between each other. Figure 13 illustrates that the Mach number ratio of linseed oil is on the top at an initial temperature of 300K. However, as the initial temperature in increasing the linseed oil is decreasing until its Mach number ratio becomes approximately the same as other fuels. Varies the initial temperature give more impact to Mach number ratio compared to increasing the mass flux.

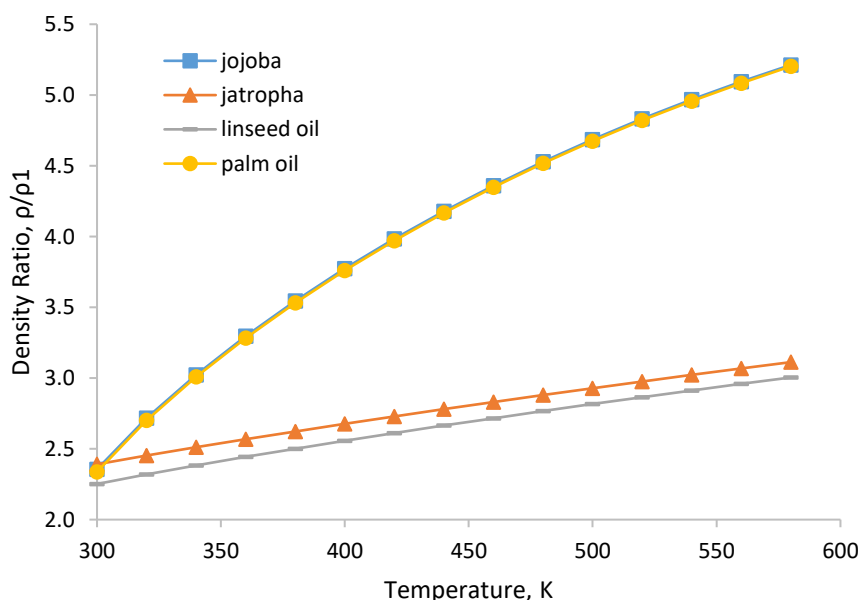


Fig. 10. Density ratio with various initial temperature

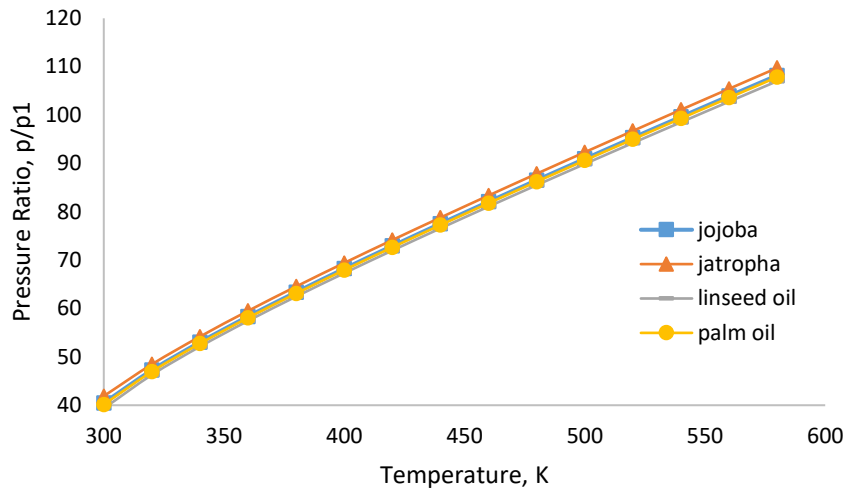


Fig. 11. Pressure ratio with various initial temperature

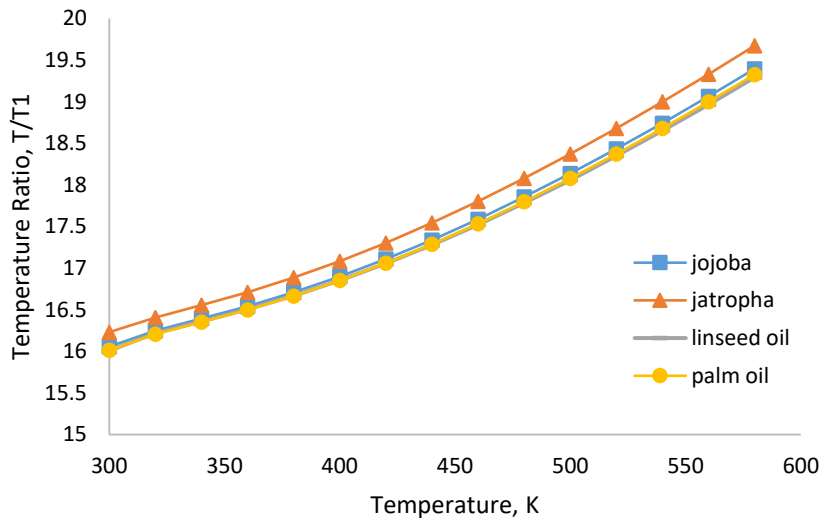


Fig. 12. Temperature ratio with various initial temperature

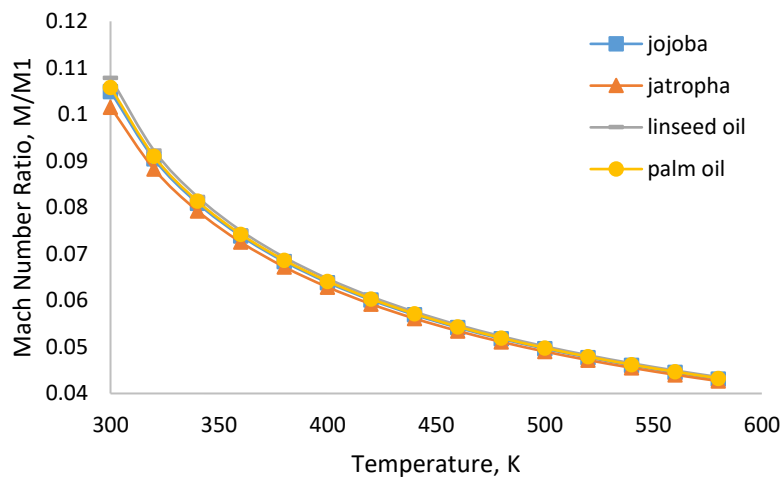


Fig. 13. Mach number ratio with various initial temperature

3.2.3 Various initial pressure

The initial pressure is varied by 300 Pa by starting at 101.3 kPa and ending at 128.9 kPa. However, the result that has been obtained is infinity at 107.3 kPa. At 107.3 kPa, as we apply the Eq. (8) it will give the value of the complex number. It shows that, the limitation of the initial pressure for detonation to occur. Therefore, the result is collected before it gives the complex number. Figure 14 shows the clear difference between each fuel used. Compared with the variation of mass flux and initial temperature, by varying the initial pressure we can see differences between each fuel. Jatropa fuel shows the highest temperature ratio, density ratio, and pressure ratio. This result shows that Jatropa is more sensitive to the change of the initial pressure compared to other fuels. In contrast, in the Mach number ratio linseed oil is at the top.

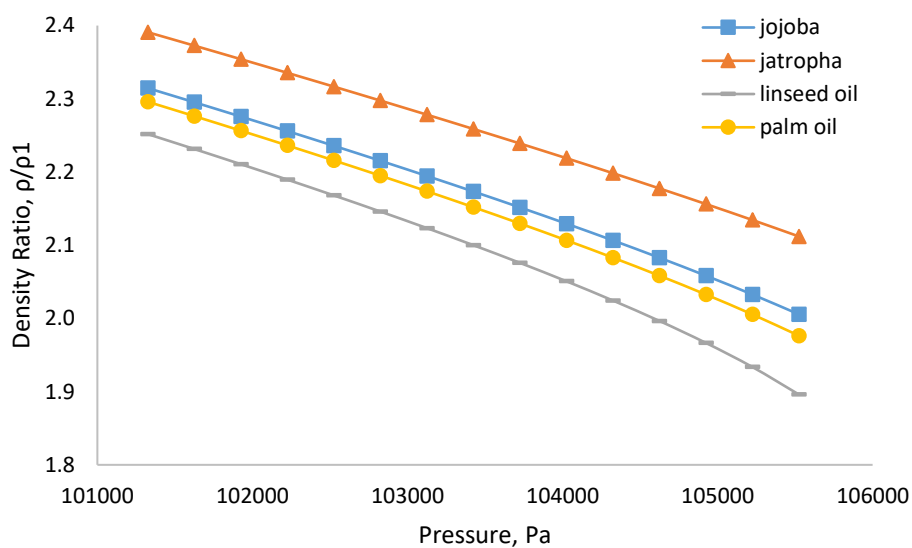


Fig. 14. Density ratio with various initial pressure

The trend of the pressure ratio and temperature ratio for all fuels is decreasing as the pressure increases, as shown in Figure 15 and 16. The Mach number ratio, on the other hand, exhibits a decreasing pattern as pressure rises in Figure 17. Figure 18 illustrates the Mach number of the burning gas under strong and weak shock conditions. The mass flux used to get the result are 5000, 6000, and 7000 kg/m²s. The initial temperature is set to 500 K, and the initial pressure is increased by 3 kPa. The trend for all values of mass flux shows the same trend which is the burn gas Mach number increase for the strong shock wave, while a weak shock tends to decrease the burned gas flow. As shown in Figure 18, although the mass flux is different, the burnt gas flow converges at the choking condition (Ma= 1).

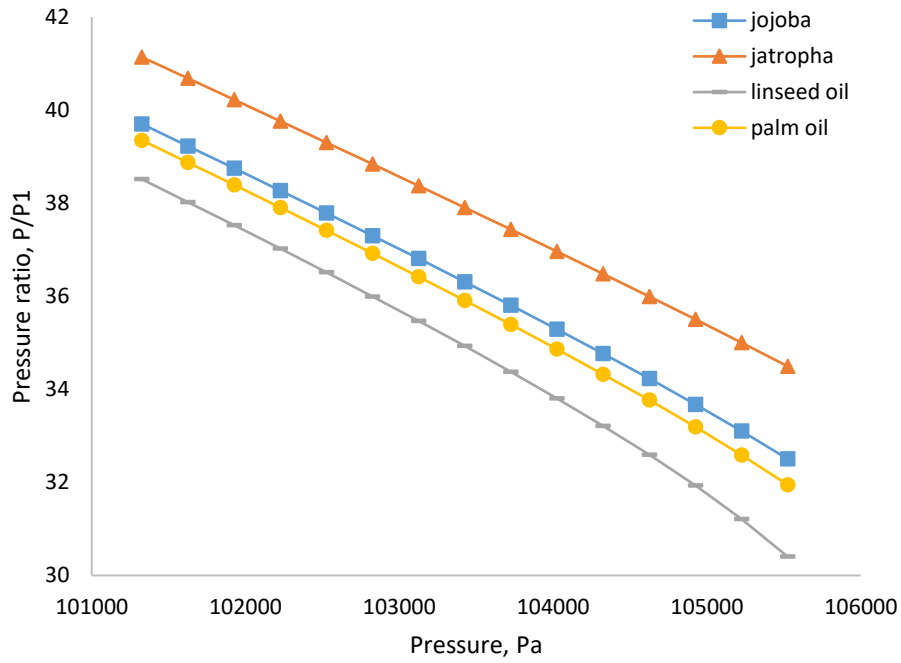


Fig. 15. Pressure ratio with various initial pressure

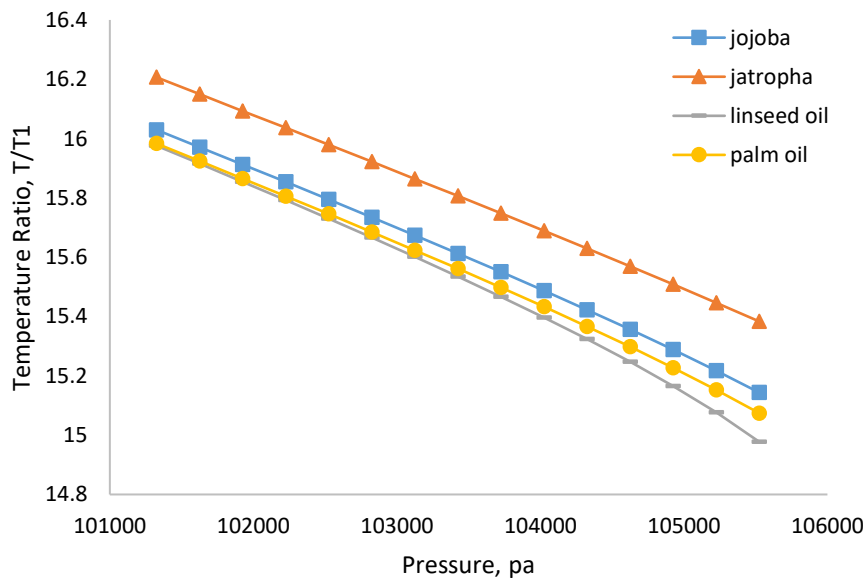


Fig. 16. Temperature ratio with various initial pressure

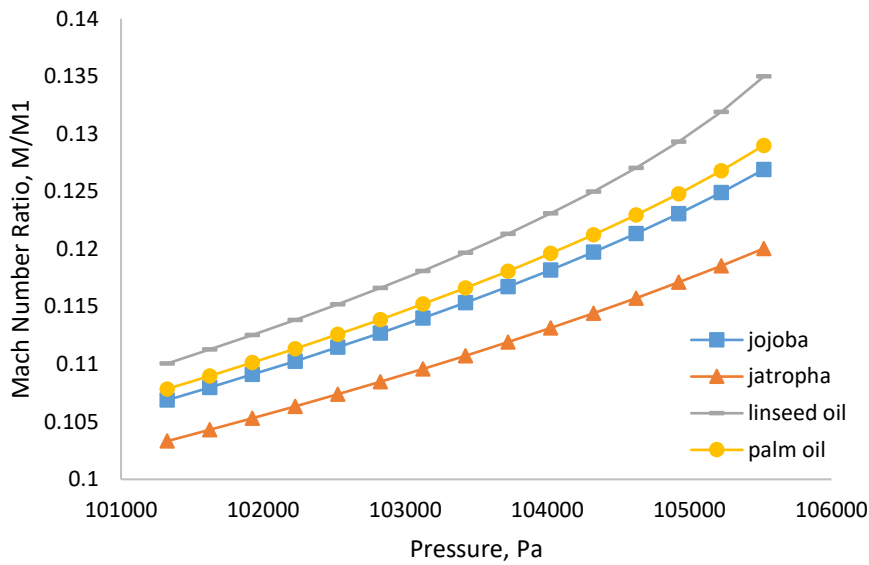


Fig. 17. Mach number ratio with various initial pressure

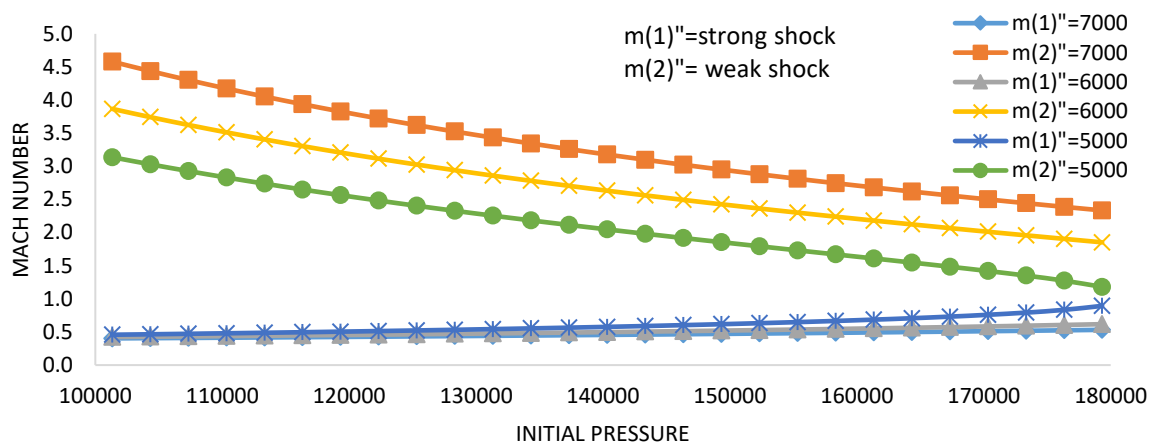


Fig. 18. The strong and weak shock of Jojoba

3.3 Humphrey and Brayton Efficiency

The Humphrey and Brayton efficiency for each fuel is calculated by using the equation from Eq. (23) and Eq. (24). To calculate this efficiency, the data from Table 11 is used. The two values of T4/T3 will produce two different values of the Humphrey and Brayton cycle.

Table 11

Properties required to calculate efficiency

| Properties | Jojoba | Jatropa | Linseed oil | Palm oil |
|------------|----------|---------|-------------|----------|
| π_c | 30.587 | 30.878 | 30.359 | 30.375 |
| T2/T3 | 0.364 | 0.363 | 0.364 | 0.363 |
| γ | 1.238239 | 1.238 | 1.237 | 1.237 |
| T4/T3 (i) | 16.05717 | 16.207 | 15.976 | 15.983 |
| T4/T3 (j) | 13.52844 | 13.538 | 13.815 | 13.669 |

Figure 19, Figure 20, and Figure 21 show that the change of the Brayton and Humphrey efficiency as we vary the mass flux, initial temperature, and initial pressure. This figure only shows the efficiency of the Jojoba oil. However, the other three oil also show the same pattern of increasing and decreasing as the variation is made.

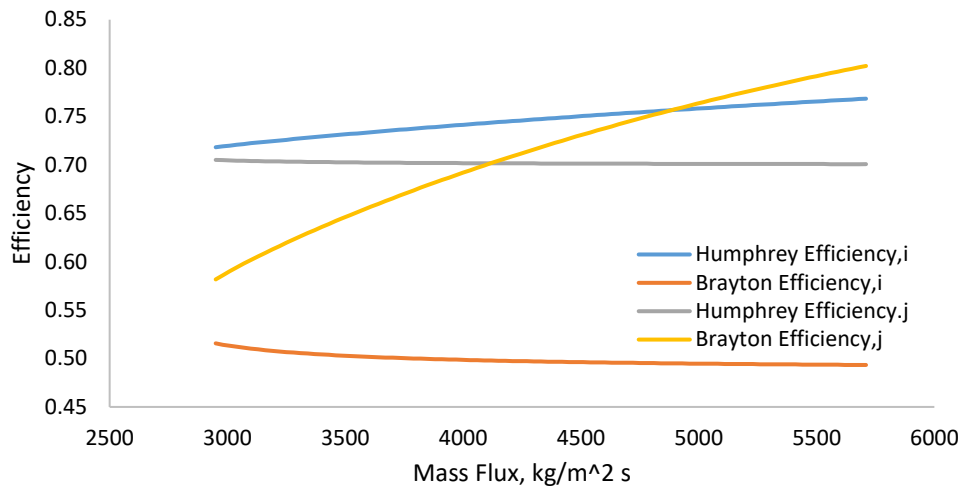


Fig. 19. Humphrey and Brayton Efficiency changing with various mass flux

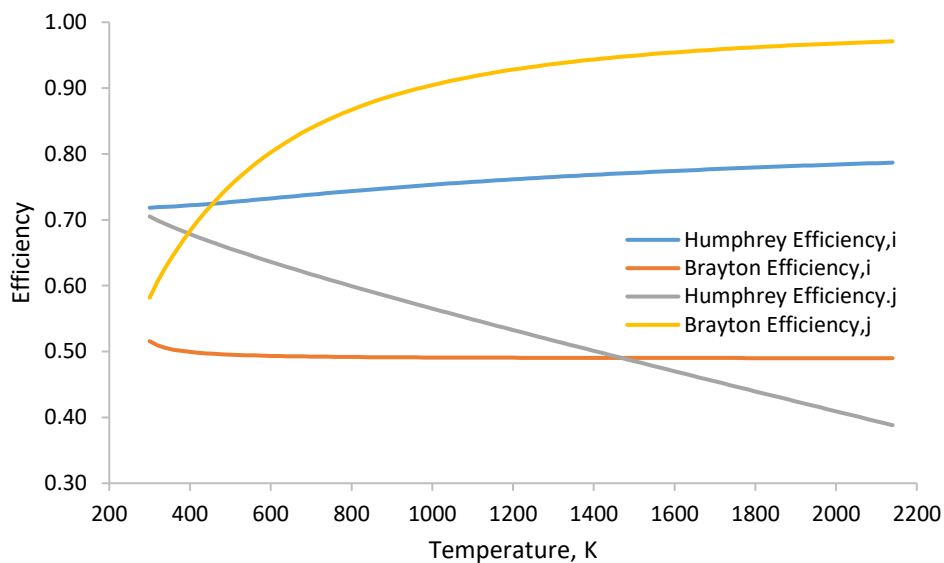


Fig. 20. Humphrey and Brayton Efficiency changing with various initial temperature

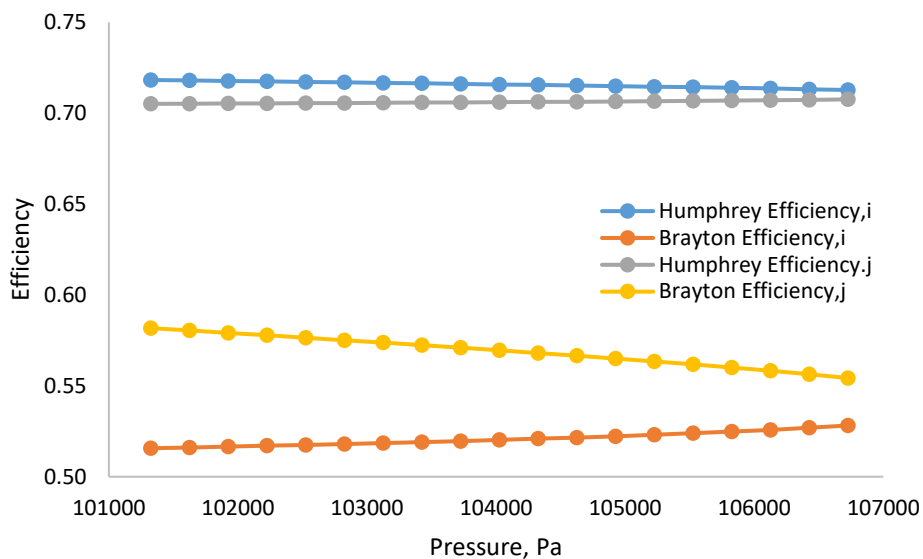


Fig. 21. Humphrey and Brayton Efficiency changing with various initial pressure

3.4 Specific Thrust and Specific Impulse

To investigate the propulsive performance of aircraft, specific thrust and specific impulse are important to show the capability of fuel as it implements in the aircraft. The input parameter ratio of the purge to the valve-open time period, β , and Mach number at unburn gas, M_1 is increasing to see the result of the specific thrust and impulse.

3.4.1 Effect of ratio of the purge to the valve-open time period, β

The purge to the valve-open time period, β is decreasing as we increase the time of the purge. By increasing the time of the cycle by 0.05 ms, it will decrease the β by 0.00182 ms. Based on Figure 22 the specific thrust is decreasing significantly after the purge to the valve-open time period, β is decreased. An aircraft that moves at subsonic speeds will be more efficient by having low specific thrust. However, it also gives a negative impact on exhaust velocity and maximum airspeed. Furthermore, the specific impulse does not show the same trend with a specific thrust. Figure 23, illustrates those specific impulses increase slightly. Generally, the higher the specific impulse, the more push that the aircraft get for the fuel used.

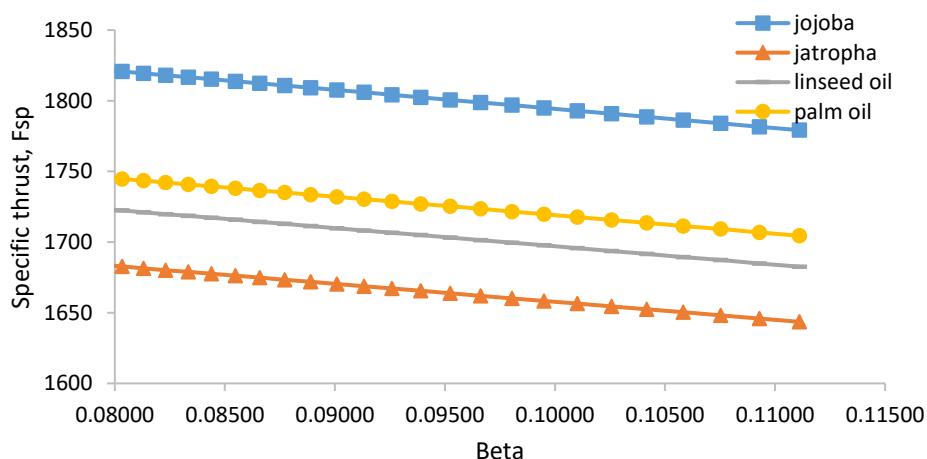


Fig. 22. Specific thrust against beta

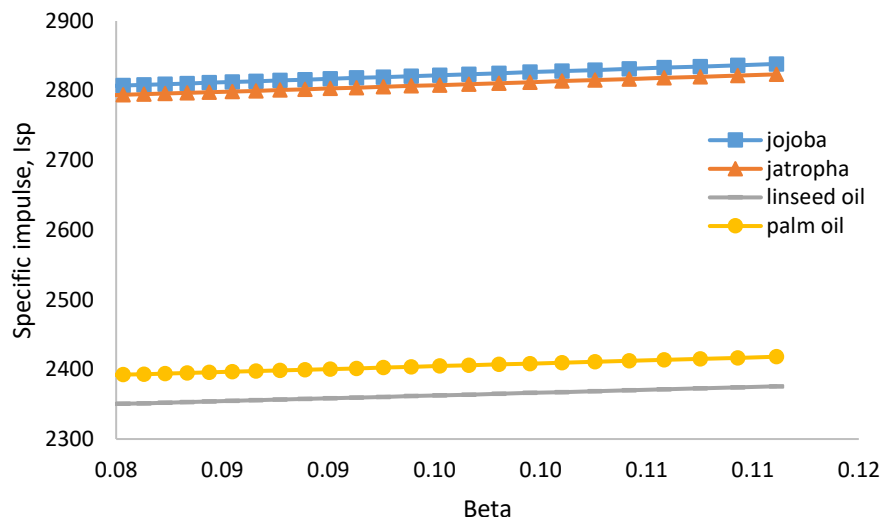


Fig. 23. Specific impulse against beta

4. Conclusions

In these studies, the propulsive performance of the biofuel is investigated to determine which biofuel has a better propulsive performance in the pulse detonation engine. By using the one-dimensional model of alternative fuel in a detonation mode, the propulsive performance and thermodynamic efficiency are being investigated. This research presents the feasibility and effectiveness of using different alternative fuels under a pulse detonation engine.

Firstly, the detonation analysis has been made by using 4 different fuels. This fuel is using the ZND model. In this section, the initial temperature is varied to determine the temperature ratio, density ratio, pressure ratio, and Mach number in three different states, which are state 1, state 2' and state 2. The result that has been obtained show that all parameter is decreased after the initial temperature is increased. Secondly, under detonation conditions, the parameter of the initial pressure, initial temperature, and mass flux is increasing to identify the impact toward the pressure, temperature, velocity, and Mach number at the C-J point. From the models that have been made, the result showed two different values for the parameter at the C-J point. One of the values is for strong shock condition and the other is weak shock condition. Figures 1,2 and 3 prove that a variety of initial pressure will decrease the pressure ratio, temperature ratio, and density ratio. However, the variation of mass flux and initial temperature give the reverse result to the variation of the pressure.

Next, from the biofuel used, the Brayton and Humphrey efficiency of each fuel has been calculated to investigate the result of using pulse detonation engine by using alternative fuel. The calculation proves that the Humphrey efficiency is higher than Brayton efficiency. Lastly, the specific impulse and specific thrust of the alternative fuel are calculated to determine the propulsive performance that can be shown from different alternative fuels. As expected, that different molecular structures will have behaviours that show their sensitivities. Furthermore, by changing the Mach number, M_1 of unburned gas, and the purge to the valve-open time period, β will affect the specific impulse and also the specific thrust. This change shows how the propulsive performance of aircraft react as there are variation in M_1 and β .

Acknowledgement

The authors would like to thank and acknowledge the Ministry of Education for Fundamental Research Grant Scheme (FRGS/1/2018/TK09/UIAM/03/3) for this research.

References

- [1] Kailasanath, K., G. Patnaik, and C. Li. "The flowfield and performance of pulse detonation engines." *Proceedings of the Combustion Institute* 29, no. 2 (2002): 2855-2862. [https://doi.org/10.1016/S1540-7489\(02\)80349-2](https://doi.org/10.1016/S1540-7489(02)80349-2)
- [2] Wu, Yuhui, Fuhua Ma, and Vigor Yang. "System performance and thermodynamic cycle analysis of airbreathing pulse detonation engines." *Journal of Propulsion and Power* 19, no. 4 (2003): 556-567. <https://doi.org/10.2514/2.6166>
- [3] Ni, Xiaodong, Chunsheng Weng, Han Xu, and Qiaodong Bai. "Numerical analysis of heat flow in wall of detonation tube during pulse detonation cycle." *Applied Thermal Engineering* 187 (2021): 116528. <https://doi.org/10.1016/j.applthermaleng.2020.116528>
- [4] Zheng, Hongtao, Qingyang Meng, Ningbo Zhao, Zhiming Li, and Fuquan Deng. "Numerical investigation on H₂/Air non-premixed rotating detonation engine under different equivalence ratios." *International Journal of Hydrogen Energy* 45, no. 3 (2020): 2289-2307. <https://doi.org/10.1016/j.ijhydene.2019.11.014>
- [5] Zhu, Yiyuan, Ke Wang, Zhicheng Wang, Minghao Zhao, Zhongtian Jiao, Yun Wang, and Wei Fan. "Study on the performance of a rotating detonation chamber with different aerospikes nozzles." *Aerospace Science and Technology* 107 (2020): 106338. <https://doi.org/10.1016/j.ast.2020.106338>
- [6] Murray, Austin P., Tyler L. Smith, Eric D. Pittman, Haiting Liu, Eric M. Crisp, Jeffrey D. Moore, and Grant A. Risha. "Frequency and Spark Timing Effects on Thrust for Pulse Detonation Engine." *Journal of Propulsion and Power* 37, no. 2 (2021): 242-251. <https://doi.org/10.2514/1.B38049>
- [7] Bhatt, M., D. Jani, and D. P. Patel. "A review on pulse detonation engine." *J Emerging Technol Innovative Res* 4 (2017): 150-153.
- [8] Deane, P., R. O. Shea, B. Ó. Gallachóir, and D. Buchholz. "Biofuels for aviation." *Insight-E Rapid Response Energy Brief* 5 (2015).
- [9] Elhawary, Shehab, Aminuddin Saat, Mazlan Abdul Wahid, and Ahmad Dairobi Ghazali. "Experimental study of using biogas in Pulse Detonation Engine with hydrogen enrichment." *International Journal of Hydrogen Energy* 45, no. 30 (2020): 15414-15424. <https://doi.org/10.1016/j.ijhydene.2020.03.246>
- [10] Li, Chiping, K. Kailasanath, and Gopal Patnaik. "A numerical study of flow field evolution in a pulsed detonation engine." In *38th Aerospace Sciences Meeting and Exhibit*, p. 314. 2000. <https://doi.org/10.2514/6.2000-314>
- [11] Yokoo, Ryuya, Keisuke Goto, Juhoe Kim, Akira Kawasaki, Ken Matsuoka, Jiro Kasahara, Akiko Matsuo, and Ikkoh Funaki. "Propulsion performance of cylindrical rotating detonation engine." *AIAA journal* 58, no. 12 (2020): 5107-5116. <https://doi.org/10.2514/1.J058322>
- [12] Watanabe, Tomohiro, Nicolas H. Jourdain, Kohei Ozawa, Nobuyuki Tsuboi, Takayuki Kojima, and Koichi A. Hayashi. "Numerical Simulation on Disk Rotating Detonation Engine: Influence of Internal Flow Field Structure on Performance." In *AIAA SciTech 2020 Forum*, p. 2160. 2020. <https://doi.org/10.2514/6.2020-2160>
- [13] Yi, Tae-Hyeong, Jing Lou, Cary Kenny Turangan, and Piotr Wolanski. "Numerical study of detonation processes in rotating detonation engine and its propulsive performance." *Transactions on Aerospace Research* (2020). <https://doi.org/10.2478/tar-2020-0015>
- [14] Dean, Anthony. "A review of PDE development for propulsion applications." In *45th AIAA aerospace sciences meeting and exhibit*, p. 985. 2007. <https://doi.org/10.2514/6.2007-985>
- [15] Wang, Ke, and Wei Fan. "Efforts on high-frequency pulse detonation engines." *Journal of Propulsion and Power* 33, no. 1 (2017): 17-28. <https://doi.org/10.2514/1.B36029>
- [16] Nikitin, V. F., V. R. Dushin, Y. G. Phylippov, and Jean Claude Legros. "Pulse detonation engines: technical approaches." *Acta Astronautica* 64, no. 2-3 (2009): 281-287. <https://doi.org/10.1016/j.actaastro.2008.08.002>
- [17] Panicker, Philip, Donald Wilson, and Frank Lu. "Operational Issues Affecting the Practical Implementation of Pulse Detonation Engines." In *14th AIAA/AHI Space Planes and Hypersonic Systems and Technologies Conference*, p. 7959. 2006. <https://doi.org/10.2514/6.2006-7959>
- [18] Coleman, M. L. *Overview of pulse detonation propulsion technology*. CHEMICAL PROPULSION INFORMATION AGENCY COLUMBIA MD, 2001.
- [19] Kaemming, T. "Integrated vehicle comparison of turbo-ramjet engine and pulsed detonation engine." *J. Eng. Gas Turbines Power* 125, no. 1 (2003): 257-262. <https://doi.org/10.1115/1.1496116>
- [20] Hoke, John, Royce Bradley, Jason Gallia, and Frederick Schauer. "The Impact of Detonation Initiation Techniques on Thrust in a Pulse Detonation Engine." In *44th AIAA Aerospace Sciences Meeting and Exhibit*, p. 1023. 2006. <https://doi.org/10.2514/6.2006-1023>

- [21] Azami, Muhammad Hanafi, and Mark Savill. "Comparative study of alternative biofuels on aircraft engine performance." *Proceedings of the Institution of Mechanical Engineers, Part G: Journal of Aerospace Engineering* 231, no. 8 (2017): 1509-1521. <https://doi.org/10.1177/0954410016654506>
- [22] Ma, Fuhua, Jeong-Yeol Choi, and Vigor Yang. "Propulsive performance of airbreathing pulse detonation engines." *Journal of Propulsion and Power* 22, no. 6 (2006): 1188-1203. <https://doi.org/10.2514/1.21755>
- [23] Turns, Stephen R. *Introduction to combustion*. Vol. 287. New York, NY, USA: McGraw-Hill Companies, 2000.